Theor Chem Acc (2011) 128:601–607
DOI 10.1007/s00214-010-0773-z

REGULAR ARTICLE

Molecular mechanism of chorismate mutase activity of promiscuos MbtI

Silvia Ferrer · Sergio Martí · Juan Andrés · Vicent Moliner · Iñaki Tuñón · Juan Bertrán

Received: 13 May 2010 / Accepted: 27 May 2010 / Published online: 15 June 2010

Abstract Salicylate synthase from Mycobacterium tuberculosis, MbtI, initiates the biosynthesis of siderophores by converting chorismate to salicylate. Nevertheless, three more distinct activities for wild-type MbtI have been detected in vitro: isochorismate synthase, isochorismate pyruvate lyase, and chorismate mutase. In this work, hybrid Quantum Mechanics/Molecular Mechanics methods have been used to get the first simulation of the chorismate mutase activity of MbtI. The results show how the reaction proceeds by means of a [3,3] sigmatropic rearrangement with free energy barrier in very good agreement with experiments. From an analysis of the averaged structures, we show that the lower chorismate mutase activity of MbtI with respect to BsCM is reflected in the lesser diaxial character of reactants in the active site. This information was used to propose the I207F mutation. The resulting free energy of activation would represent an enhancement of the rate constant by a factor of 7 at 310 K.

Published as part of the special issue celebrating theoretical and computational chemistry in Spain.

S. Ferrer · S. Martí · J. Andrés · V. Moliner (✉)
Departament de Química Física i Analítica,
Universitat Jaume I, 12071 Castelló, Spain
e-mail: moliner@uji.es

V. Moliner
Institute of Applied Radiation Chemistry,
Technical University of Lodz, 90-924 Lodz, Poland

I. Tuñón (✉)
Departament de Química Física,
Universitat de València, 46100 Burjassot, Spain

J. Bertrán
Departament de Química, Universitat Autònoma de Barcelona,
08193 Bellaterra, Spain

Keywords MbtI · Chorismate mutase activity · QM/MM · PMF · Reaction mechanism

1 Introduction

Nowadays, it is widely accepted that theoretical calculations, in combination with experimental observations, provide one of the essential tools to establish the reaction mechanism of a particular reaction. During last years, combination of Quantum Mechanics and Statistical Mechanics techniques has extended the applicability of Computational Chemistry to the analysis of reaction mechanisms in complex environments such as enzymatic processes. In this regard, the chorismate to prephenate rearrangement, or chorismate mutase (CM) activity, has been used by many scientists as a benchmark to test different techniques to get insights into the origin of enzyme catalysis [1]. The main reason for this reaction being so popular is due to the fact that it has its counterpart in solution. Theoretical calculations have clearly established that the reaction proceeds through a pericyclic rearrangement [1]. This is an additional advantage presented in this reaction, since no covalent bonds are formed between the substrate and the protein, avoiding technical problems of frontier treatments in hybrid Quantum Mechanics/Molecular Mechanics (QM/MM) schemes.

Traditionally, pericyclic reactions have been considered as a rarely exploited mechanism in cellular metabolism, despite their broad utility in the laboratory [2]. In fact, in addition to the Claisen rearrangement of chorismate to prephenate [3], just a few examples of this kind of reactions have been considered to be catalyzed by enzymes

such as the suprafacial [1, 5]-sigmatropic shift of a methyl group in the transformation of precorrin-8x to hydrogenobyrinic acid [4], and several putative Diels–Alder reactions [5].

Salicylate synthase from *Mycobacterium tuberculosis*, MbtI, is a member of the chorismate-utilizing enzymes referred to as MST family [6] that initiates the biosynthesis of small iron-chelating molecules called siderophores by converting chorismate to salicylate [2, 7–10]. Salicylate-derived siderophores as pyochelin, mycobactin, and yersinianbactin are virulence factors required for the establishment and maintenance of many infections [7]. These natural products are excreted into the extracellular environment of hosts, binding ferric ions with high affinity and transported back into bacterial cytoplasm, where the iron is released [11]. MST is an intriguing Mg^{2+}-dependent family descended from a common ancestor. Thus, for instance, while *M. tuberculosis* uses a single enzyme to synthesize salicylate, in *Pseudomonas* species, salicylate is formed by the combined activity of isochorismate synthase, PchA, and isochorismate pyruvate lyase, PchB [9, 10]. Moreover, four distinct activities for wild-type MbtI have been detected in vitro [12]. These are isochorismate synthase, isochorismate pyruvate lyase, salicylate synthase, and chorismate mutase; the first three activities requiring the presence of Mg^{2+} while the last one is observed for wild type in the absence of this cation in its active site (see Scheme 1). Nevertheless, these results have been recently questioned by Ziebart and Toney, who have found that, after doubly purification, the CM activity was abolished or significantly reduced [13]. Isochorismate synthase, isochorismate pyruvate lyase, and salicylate synthase activities seem to be also modulated by the pH of the medium, since using ^{1}H-NMR, UV–Vis spectroscopy, and HPLC analysis of reaction mixtures, accumulation of isochorismate was detected at pH values below 7.5 while the primary product at pH 8 was salicylate. The key role of pH can be related with the ionization state of the active site residues and the molecular mechanisms employed by the enzyme to catalyze the different reactions. In particular, His398 is the proposed amino acid to act as a base that abstract the C2 proton leading to pyruvate elimination; at lower pH, this histidine would be protonated and the proton abstraction process does not take place, thus explaining the experimental observation [12]. Nevertheless, the observation that wild-type MbtI and five different mutants possess CM activity in absence of Mg^{2+} was used by Zwahlen et al. [12] to propose that pyruvate elimination by MbtI takes place by a sigmatropic mechanism similar to that recently proposed for the isochorismate pyruvate lyase from *Pseudomonas aeruginosa*, PchB [2, 8, 14]. In this regard, we have recently proved the pericyclic mechanism of pyruvate elimination from isochorismate catalyzed by PchB by means of hybrid QM/MM Molecular Dynamics (MD) studies [15].

From kinetic studies, it has been proved that the different activities of wild-type MbtI in presence and absence of Mg^{+2} are comparable, with rate constants values of the same order of magnitude [12], not concluding which is the primary and secondary activities. In this sense, the chorismate mutase activity has been observed in MbtI despite the low primary amino acid sequence pairwise similarity of MbtI with chorismate mutases of reported crystal structures [6, 12, 16].

In the present work, we are studying the chorismate to prephenate rearrangement in the active site of MbtI to elucidate whether the reaction is catalyzed or not by this enzyme and to check whether it proceeds by means of a pericyclic mechanism, as proposed Zwahlen et al. [12]. The theoretical results will be tested by means of the effect of an amino acid exchange on the k_{cat} of the catalyzed reaction. The results will be used to shed some light into the atomic details of this member of the MTS family.

2 Computing methods

Our model starts from the X-ray structure of MbtI (2I6Y), crystallized in absence of Mg^{2+} [12], which has no substrate or inhibitor in the active site. Optimal position for a total of 14 missing residues has been obtained by means of successive minimization and molecular dynamic simulations on this section of the backbone where the amino acids have been added using the known sequence of MbtI. Hydrogen atoms were added using fDYNAMO [17], according to the pK_a values of the titratable amino acids of the enzyme calculated within the empirical *propKa* program of Jensen et al. [18]. Then, a total of 15 counter ions (Na^+) were placed into optimal electrostatic positions around the protein, in order to obtain electro neutrality. Finally, the full system was placed in a 79.5 Å of side box of water molecules, erasing all those water molecules with an oxygen lying less than 2.8 Å from any non-hydrogen atom. The substrate was described using Quantum Mechanics (QM) by means of the AM1 semiempirical hamiltonian [19], while for the rest of the system, we employed the molecular mechanics (MM) OPLS-AA [20] and TIP3P force fields [21], with a cutoff radius for the non-bonded interactions of 14.5 Å. The resulting structure was used to perform rigid QM/MM docking of a transition structure (TS) of the chorismate to prephenate rearrangement previously located into the active site of BsCM [22]. Among the different generated structures, only those with proper hydrogen-bonding interactions between the substrate and protein residues were kept. Using the fDYNAMO library, the selected structures were relaxed; all of them

Scheme 1 Reactions catalyzed by wild-type MbtI

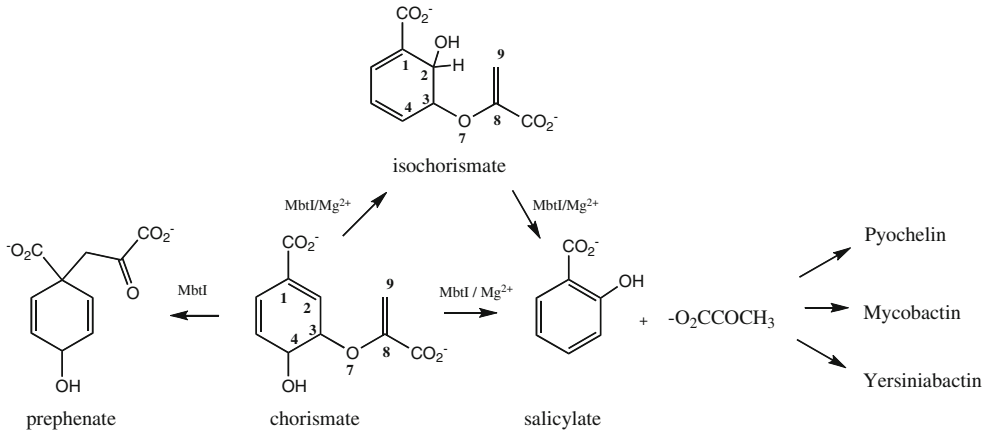

leading to a similar arrangement of the substrate in the active site. Then, starting from the lowest energy configuration, the transition structure was located and characterized including the effect of the full flexible environment using a micro–macro iteration method [23]. I207F mutant was then produced from this final structure, replacing original amino acid residues by their counterparts. All our computational models were then equilibrated at 310 K during 500 ps using the NVT ensemble and the Langevin–Verlet integrator.

Potentials of mean force (PMF) were obtained as a function of a distinguished reaction coordinate (ζ) defined as the antisymmetric combination of the bond-breaking (C3-O7) and bond-forming (C1–C9) distances (see Scheme 2), as used in previous computational studies of chorismate rearrangement [1]. An umbrella sampling approach was used by means of parabolic potentials with a force constant of 2,500 kJ mol^{-1} Å^{-1} to restraint this coordinate at particular values covering the range between reactants and products. This required series of 70 simulation windows. Each of these windows consisted in 5 ps of equilibration and 10 ps of production, with a time step of 1 fs. Weighted histogram analysis method (WHAM) was then used to obtain the full probability distribution function [24, 25].

Finally, in order to correct the low-level AM1 energy function used in the PMF, an interpolated correction scheme developed in our laboratory has been applied [26]. In this correction scheme, based on a method proposed by Truhlar et al. for dynamical calculations of gas phase chemical reactions [27], the new energy function employed in the simulations is defined as:

$$E = E_{\mathrm{LL/MM}} + S\left[\Delta E_{\mathrm{LL}}^{\mathrm{HL}}(\zeta)\right] \quad (1)$$

where S denotes a spline function, whose argument $\Delta E_{\mathrm{LL}}^{\mathrm{HL}}(\zeta)$ is a correction term taken as the difference between single-point calculations of the QM subsystem using a high-level (HL) method, in this case, the hybrid functional B3LYP [28, 29] with the 6-31G* basis set, and the low-level (LL) one, the AM1 hamiltonian. The correction term is expressed as a function of the distinguished reaction coordinate ζ.

3 Results and discussion

The transformation of chorismate into prephenate is a Claisen rearrangement involving a C3-O7 bond-breaking and C1–C9 bond-forming processes (see Scheme 2). This reaction takes place through a diaxial TS and is preceded by a conformational equilibrium between non-reactive pseudo-diequatorial and reactive pseudo-diaxial chorismate conformers, the last one being closer to the TS. It has been proposed that the catalytic character of chorismate mutases comes from an electrostatic stabilization of the TS and the preferential stabilization of reactive chorismate conformers. Both effects are obviously connected and related to the protein structure [1, 15, 30–32].

In order to study the chorismate to prephenate rearrangement catalyzed by MbtI, and as described in previous

Scheme 2 Chorismate to prephenate rearrangement

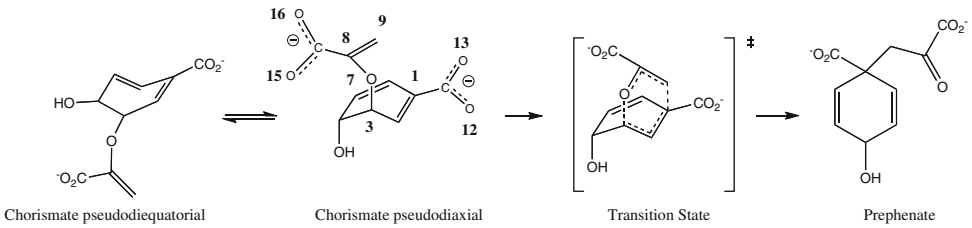

section, the free energy profile has been computed in terms of the PMF, using the antisymmetric combination of distances describing breaking and forming bonds as the distinguished reaction coordinate. The result is depicted in Fig. 1, where the AM1/MM PMFs of the uncatalyzed reaction in solution and the profile of the reaction catalyzed by one of the most efficient chorismate mutase enzyme, the *Bacillus subtilis* CM (BsCM) [22], are also presented for comparison purposes. As it can be observed in the figure, the lowest free energy barrier profile is obtained for BsCM, while the highest activation free energy is obtained in solution and the MbtI rendering a value in between. The differences between the uncatalyzed reaction and the two catalyzed reactions, by BsCM and MbtI, are 8.7 and 3.8 kcal mol^{-1}, respectively. Thus, our results predict that the catalytic rate constant for the CM activity of MbtI would be about 4,000 times lower than for BsCM. These results are in very good agreement with the values deduced from the experimentally measured rate constants [33, 34], from which activation free energy differences of 9.1 and 4.7 kcal mol^{-1} can be obtained applying Transition State Theory (TST) in its simplest version. Note that the BsCM and in solution reactions have been studied at 300 K, while the MbtI was studied at 310 K, both theoretically and experimentally. From the free energy barriers reported in Table 1, it is observed how the absolute values computed at the AM1/MM level are, by comparison with the experimental data, overestimated, although a good agreement have been shown for the relative values of the barriers. The errors in the absolute values are dramatically reduced when corrections obtained at the B3LYP level are included (see Table 1), confirming the reliability of our method and results to describe the molecular mechanism of CM activity of MbtI.

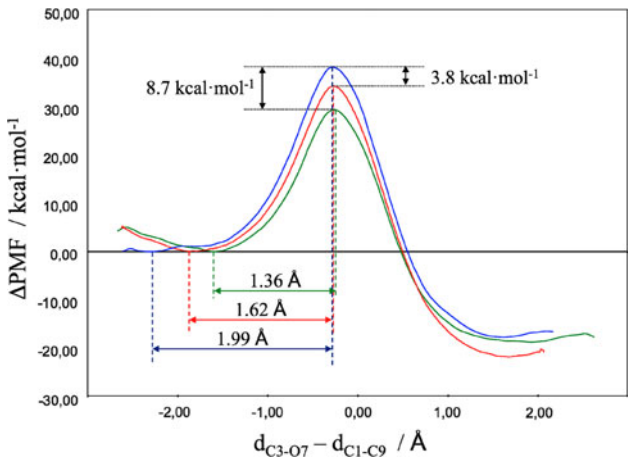

Fig. 1 Free energy profiles, computed in terms of PMF, for the chorismate to prephenate rearrangement in aqueous solution (*blue line*) and catalyzed by the BsCM (*green line*) and by the MbtI (*red line*)

Table 1 Activation free energies obtained at AM1/MM and corrected at B3LYP:AM1/MM level, together with values calculated from experimentally measured rate constants, for the chorismate to prephenate rearrangement in the different media

	$\Delta PMF^{\ddagger}_{AM1/MM}$	$\Delta PMF^{\ddagger}_{B3LYP:AM1/MM}$	$\Delta G^{\ddagger}_{exp}$
Water	38.0[a]	27.8	24.5[c]
BsCM	29.3[a]	19.8[b]	15.4[d]
MbtI	34.2	24.8	19.8[e]

All values are reported in kcal mol^{-1}

[a] From Ref. [22]

[b] From Ref. [26]

[c] From Ref. [33]

[d] From Ref. [34]

[e] From Ref. [12]

The averaged bond-breaking and bond-forming distances in the TS show that the reaction proceeds through a concerted but asynchronous process, being the TS structures very similar both in BsCM and MbtI (see Table 2). Nevertheless, important differences are obtained in the reactants state. As observed in Table 2, C1–C9 distance in the reactant states are 3.75, 3.05, 3.30 Å in water, BsCM and MbtI, respectively, providing information on the reactive character of the reactants: large C1–C9 distances correspond to non-reactive pseudo-diequatorial conformer while shorter distances are associated with reactive pseudo-diaxial forms. According to these results, it seems that BsCM enzyme is pushing the ether bridge to the ring rendering more diaxial character conformers [30, 31], while in solution, reactants molecules are preferentially found in the pseudo-diequatorial conformation. Reactants obtained in the active site of MbtI present a more diaxial character than those obtained solution, but still far from the values found in the Michaelis complex of BsCM. These features can be also deduced from analysis of the differences in the reaction coordinate between reactants and TS displayed in Fig. 1, where the value in the MbtI appears in between BsCM and aqueous solution results. Furthermore, the distance between the two carboxylate groups in the chorismate molecule is larger in solution (6.58 Å) than in the BsCM (5.61 Å). MbtI render values that are also shorter than in solution (5.65 Å). The chorismate conformations found in solution are dominated by the electrostatic repulsion between the two carboxylate groups, while in the enzymes, these distances are closer, thus suggesting that the energy penalty associated to the approach of two negatively charged groups must be compensated by intermolecular interactions with residues of the active site. These interactions favor the population of chorismate pseudo-diaxial conformer in the enzymatic environments.

An analysis of the specific protein–substrate interactions has been done in reactants and in the TS. A detailed analysis

Table 2 Averaged distances obtained for R and TS in aqueous solution and in the enzymatic environments for the chorismate rearrangement obtained at AM1/MM level

	Water[a]		BsCM[a]		MbtI		MbtI I207F	
	R	TS	R	TS	R	TS	R	TS
d_{C3-O7}	1.45 ± 0.03	1.78 ± 0.02	1.45 ± 0.03	1.94 ± 0.02	1.44 ± 0.03	1.93 ± 0.02	1.44 ± 0.03	2.05 ± 0.02
d_{C1-C9}	3.75 ± 0.20	2.09 ± 0.10	3.05 ± 0.18	2.18 ± 0.09	3.30 ± 0.18	2.17 ± 0.02	3.25 ± 0.17	2.33 ± 0.02
$d_{CO2-CO2-}$	6.58 ± 0.23	4.87 ± 0.16	5.61 ± 0.28	4.89 ± 0.15	5.65 ± 0.16	5.05 ± 0.11	5.59 ± 0.16	5.02 ± 0.12

All values are reported in Å

[a] From Ref. [21]

of averaged structures on both states reveals that the most strong interactions are established between the carboxylate and ether oxygen atoms of the substrate and four amino acids of the active site. These four amino acids are three lysines (Lys205, Lys293, and Lys438) and one arginine (Arg405); the three lysines are at hydrogen bond distances from the carboxylate moieties, while the Arg405 is interacting with one of the carboxylate groups and with the ether oxygen atom. This oxygen atom (O7) is also interacting with a water molecule located in the active site pocket. Figure 2 corresponds to a representative snapshot of the TS where distances have been averaged along the last 500 ps of the corresponding constrained trajectory. The substrate–protein pattern of interactions observed in reactants is qualitatively equivalent to the one observed in the TS (see Table 3). It is important to point out that, by comparison with the same analysis carried out in the TS of the BsCM [22], it seems that TS structures located in MbtI are less strongly bounded than in BsCM. Four arginine residues (Arg7, Arg63, Arg90, and Arg116) were at standard hydrogen bond distances from the oxygen atoms of the carboxylate in BsCM. In particular, the averaged distance of Arg90 to the ether bridge of the TS in BsCM is reduced from the reactant state to the TS (from 2.66 to 2.21 Å) while the equivalent distance between Arg405 and the same ether oxygen atom of the substrate in MbtI is increased from the reactants to the TS (from 2.68 to 2.86 Å) [22, 31, 32]. This interaction was estimated to contribute about 3 kcal mol^{-1} to the free energy barrier lowering in BsCM with respect to the uncatalyzed reaction [32], and thus it can also account for the reduced CM activity of MbtI. The different TS stabilization by the protein–substrate binding between BsCM and the MbtI seems to be responsible of the different chorismate mutase catalytic efficiency between both enzymes.

4 Mutations

An exhaustive analysis of the substrate–protein interactions at a molecular level allows proposing *in silico*

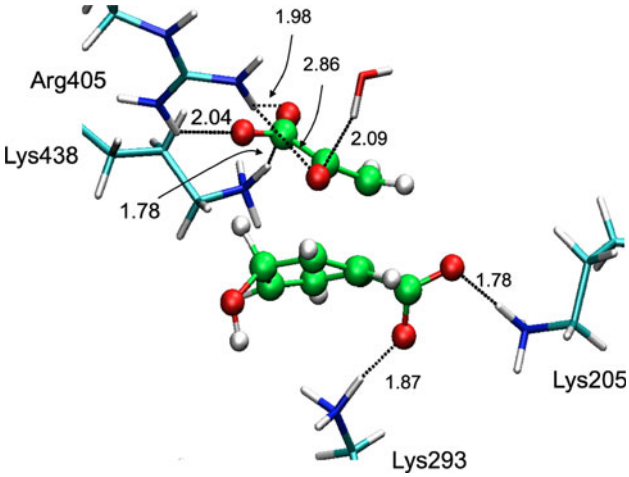

Fig. 2 Snapshot representative of the TS of the chorismate to prephenate rearrangement obtained in the active site of the MbtI. Key averaged distances are reported in Å

mutations in order to explain the origin of the change in the k_{cat} of the catalyzed reaction. In this sense, once established that the low chorismate mutase activity of the MbtI is reflected in the lesser diaxial character of the reactants in the active site, the 207 position initially occupied by an isoleucine has been exchanged by a phenylalanine, a much larger amino acid which, presumably, should be translated into a more constrained substrate, thus keeping the ether bridge into a more diaxial conformation and then favoring population of more reactive conformations. Our simulations show how this I207F mutation renders a diminution of the active site volume by about 13% (using a probe radius of 1.4 Å, we estimated that the averaged volumes of the active sites are 542 and 470 $Å^3$ for wild type and mutant, respectively). The resulting averaged structure after performing this mutation is shown in Fig. 3, where superposition of reactant structures of wild type and mutant is presented, and in Table 2, where averaged values of key distances are listed. As observed, the two carbon atoms to be bounded, C1 and C9, appear at a shorter distance in the mutant than in the wild type (3.25 and 3.30 Å, respectively).

Table 3 Averaged hydrogen bond distances between substrate atoms and protein residues obtained for R and TS in the wild-type MbtI environments for the chorismate rearrangement at AM1/MM level

	MbtI		MbtI I207F	
	R	TS	R	TS
O7-Arg405	2.68 ± 0.24	2.86 ± 0.24	2.83 ± 0.25	2.87 ± 0.24
O7-wat	2.06 ± 0.14	2.09 ± 0.16	2.20 ± 0.24	2.20 ± 0.18
O12-Lys205	1.77 ± 0.12	1.78 ± 0.12	1.76 ± 0.11	1.81 ± 0.12
O13-Lys293	1.90 ± 0.15	1.87 ± 0.14	1.94 ± 0.17	1.95 ± 0.17
O15-Lys438	1.88 ± 0.15	1.78 ± 0.12	1.86 ± 0.15	1.77 ± 0.12
O16-Arg405(HH21)	2.04 ± 0.18	1.98 ± 0.16	2.05 ± 0.18	2.01 ± 0.17
O16-Arg405 (HH11)	1.92 ± 0.14	2.04 ± 0.17	1.86 ± 0.12	1.91 ± 0.13

All values are reported in Å

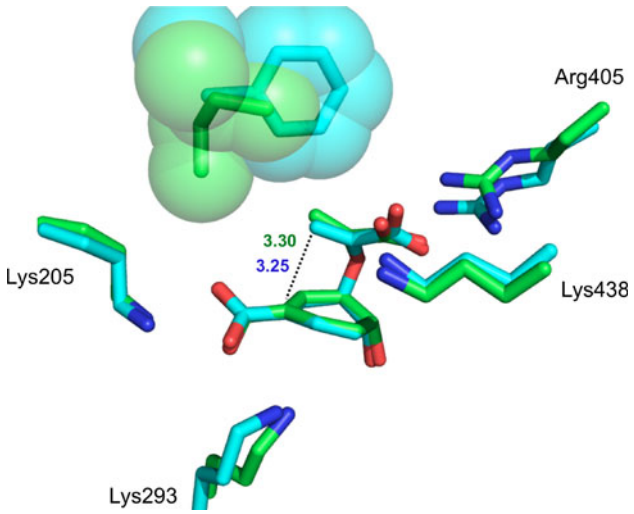

Fig. 3 Superposition of averaged reactant structures of the wild-type MbtI and the I207F mutant, where the original residue Ile207 is colored in *green* while the mutated phenylalanine is colored in *blue*. Averaged C1–C9 distances are reported in Å

Another interesting effect of the I207F mutation is observed in the behavior of the O7-Arg405 interaction (see Table 3). Thus, while this distance is substantially increased from reactants to the TS in the wild-type enzyme (from 2.68 to 2.86 Å), in the mutant, this distance remains almost unchanged (from 2.83 to 2.87 Å). Keeping in mind that, as mentioned above, the interaction between an arginine residue (Arg90) and the ether oxygen stabilized the TS with respect to reactants in the BsCM [22, 31, 32], and considering that similar charge on O7 is obtained in reactants and TS in wild type and I207F, the smaller change of O7-Arg405 distance from reactants to the TS of the later would contribute to reduce the free energy barrier with respect to the wild type. Obviously, the lengthening of the O7-Arg405 distance in the Michaelis complex could also lead to a slight increase in K_M.

The obtained AM1/MM PMF for the I207F mutant supports our predictions; the free energy barrier is now 33.0 kcal mol^{-1}, which represents 1.2 kcal mol^{-1} lower than the obtained in wild-type MbtI. In accordance with our previous analysis (see Table 2), the difference between the reaction coordinates in reactants and in the TS in the I207F mutant (1.53 Å) appears significantly reduced with respect to the value obtained for the wild-type MbtI (1.62 Å).

5 Conclusions

QM/MM MD methods have been used to get the first simulation of the chorismate mutase activity of the wild-type MbtI. Free energy of activation has been obtained from the PMF, and the results have been compared with the reference reaction in solution and with the catalyzed reaction in the *Bacillus subtilis* Chorismate Mutase (BsCM). The results show how the reaction in MbtI proceed by means of a [3,3] sigmatropic rearrangement with a free energy barrier that is in between the one obtained in solution and the one obtained for the BsCM. The free energy barrier obtained for the reaction in MbtI was 3.8 kcal mol^{-1} lower than in aqueous solution, while the experimental difference (deduced from rate constants in the context of the TST) is 4.7 kcal mol^{-1}. On the other side, the estimated free energy barrier for MbtI was 4.9 kcal mol^{-1} higher than in BsCM, while the estimation based on experimental rate constants is of 4.4 kcal mol^{-1}, thus confirming the reduced CM activity of MbtI relative to BsCM. From an analysis of the averaged structures of reactants and transition state, the lower chorismate mutase activity of the MbtI has been postulated to be reflected in the lesser diaxial character of the reactants in the active site. This result has motivated a search for a mutation that increased the chorismate mutase activity by increasing the diaxial character of the substrate, rendering a lower free energy barrier. In this regard, a phenylalanine has been placed in the 207 position initially occupied by an isoleucine. This I207F mutation renders an important diminution of the active site volume which was translated into a more constrained substrate thus keeping the ether bridge into a more diaxial conformation. The resulting free energy of activation for the I207F mutant was 1.2 kcal mol^{-1} lower than for the wild-type MbtI, which would represent an enhancement of the rate constant by a factor of 7 at 310 K.

This study shows how computational techniques can be used to obtain mechanistic information of enzyme-catalyzed reaction at molecular level. This information can be used to predict mutations that improve the catalytic efficiency thus providing a valuable tool to assist molecular engineering.

Acknowledgments We thank the Spanish Ministry *Ministerio de Ciencia e Innovación* for project CTQ2009-14541-C02, Universitat Jaume I—BANCAIXA Foundation for projects P1.1B2008-36, P1.1B2008-37 and P1.1B2008-38, and Generalitat Valenciana for *Prometeo*/2009/053 project. The authors also acknowledge the Servei d′Informatica, Universitat Jaume I for generous allotment of computer time. V. Moliner also thanks the Spanish Ministry *Ministerio de Educación* for traveling financial support, project PR2009-0539.

References

1. Martí S, Roca M, Andrés J, Moliner V, Silla E, Tuñón I, Bertrán J (2004) Chem Soc Rev 33:98–107
2. DeClue MS, Baldridge KK, Kunzler DE, Kast P, Hilvert D (2005) J Am Chem Soc 127:15002–15003
3. Chook YM, Ke H, Lipscomb WN (1993) Proc Natl Acad Sci USA 90:8600–8603
4. Li Y, Alanine AID, Vishwakarma RA, Balachandran S, Leeper FJ, Battersby AR (1994) Chem Comm 2507–2508
5. Stocking EM, Williams RM (2003) Angew Chem Int Ed 42:3078–3115
6. Kolappan S, Zwahlen J, Zhou R, Truglio JJ, Tonge PJ, Kisker C (2007) Biochemistry 46:946–953
7. Crosa JH, Walsh CT (2002) Microbiol Mol Biol Rev 66:223–251
8. Wright SK, DeClue MS, Mandal A, Lee L, Wiest O, Cleland WW, Hilvert D (2005) J Am Chem Soc 127:12957–12964
9. Gaille C, Kast P, Haas D (2002) J Biol Chem 277:21768–21775
10. Gaille C, Reimmann C, Haas D (2003) J Biol Chem 278:16893–16898
11. Cisar JS, Tan DS (2008) Chem Soc Rev 37:1320–1329
12. Zwahlen J, Kolappan S, Zhou R, Kisker C, Tonge PJ (2007) Biochemistry 46:954–964
13. Ziebart KT, Toney MD (2010) Biochemistry 49:2851–2859
14. Kunzler D, Sasso S, Gamper M, Hilvert D, Kast P (2005) J Biol Chem 280:32827–32834
15. Martí S, Andrés J, Moliner V, Silla E, Tuñón I, Bertrán J (2009) J Am Chem Soc 131:16156–16161
16. Harrison AJ, Yu M, Gardenborg T, Middleditch M, Ramsay RJ, Baker EN, Lott JS (2006) J Bacteriol 188:6081–6091
17. Field MJ, Albe M, Bret C, Proust-De Martin F, Thomas A (2000) J Comp Chem 21:1088–1100
18. Li H, Robertson AD, Jensen JH (2005) Proteins 61:704–721
19. Dewar MJS, Zoebisch EG, Healy EF, Stewart JJP (1985) J Am Chem Soc 107:3902–3909
20. Jorgensen WL, Maxwell DS, TiradoRives J (1996) J Am Chem Soc 118:11225–11236
21. Jorgensen WL, Chandrasekhar J, Madura JD, Impey RW, Klein ML (1983) J Chem Phys 79:926–935
22. Martí S, Andrés J, Moliner V, Silla E, Tuñón I, Bertrán J, Field MJ (2001) J Am Chem Soc 123:1709–1712
23. Martí S, Moliner V, Tuñón I (2005) J Chem Theory Comp 1:1008–1016
24. Kumar S, Bouzida D, Swendsen RH, Kollman PA, Rosenberg JM (1992) J Comp Chem 13:1011–1021
25. Torrie GM, Valleau JP (1977) J Comp Phys 23:187–199
26. Ruiz-Pernia JJ, Silla E, Tuñón I, Martí S, Moliner V (2004) J Phys Chem B 108:8427–8433
27. Chuang YY, Corchado JC, Truhlar DG (1999) J Phys Chem A 103:1140–1149
28. Miehlich B, Savin A, Stoll H, Preuss H (1989) Chem Phys Lett 157:200–206
29. Becke AD (1993) J Chem Phys 98:5648–5652
30. Martí S, Andrés J, Moliner V, Silla E, Tuñón I, Bertrán J (2000) J Phys Chem B 104:11308–11315
31. Martí S, Andrés J, Moliner V, Silla E, Tuñón I, Bertrán J (2003) Chem Eur J 9:984–991
32. Martí S, Andrés J, Moliner V, Silla E, Tuñón I, Bertrán J (2004) J Am Chem Soc 126:311–319
33. Andrews PR, Smith GD, Young IG (1973) Biochemistry 12:3492–3498
34. Kast P, AsifUllah M, Hilvert D (1996) Tetra Lett 37:2691–2694